Academic Article

Influence of Heat Transport by Sea Breezes on Inland Temperature in the Osaka Area

Atsumasa Yoshida*[1] Junichi Yashiro*[1] Xinbo Xiao*[1] Ryusuke Yasuda*[1]

*[1] Department of Mechanical Engineering, Osaka Prefecture University

Corresponding author: Atsumasa YOSHIDA, ayoshida@me.osakafu-u.ac.jp

ABSTRACT

Heat transport from Osaka city to inland areas by sea breezes in mid-summer was evaluated using a mesoscale meteorological model. The magnitude of the advection, diffusion, and radiation terms in the conservation equation of potential temperature was individually evaluated.

The advection term was found to always show a cooling effect, and its magnitude and time variation were similar to the diffusion term, but with opposite sign. The cooling effect of the advection term decreases from the coastal area to the inland area, but hardly turns to heating. Another simulation of increasing the anthropogenic heat in Osaka city area was executed and the results show that heat transport from the central area by sea breezes does not lead to temperature rise in the inland area.

Key Words : Urban heat island, Sea breeze, Heat advection, Numerical model

1. Introduction

In Osaka, the most populous city in western Japan, and in other Japanese megacities, such as Tokyo and Nagoya, countermeasures to the urban heat island (UHI) problems in summer are an important issue. Based on the "wind passage" concept, the local government of Osaka city has created a future urban plan for the area[(1)] to utilize the cooling potential of sea breezes. In the plan, widening of streets and the creation of open spaces along the paths of sea breezes are proposed to promote ventilation in the city; however, it has been pointed out by some researchers that the UHI of megacities causes temperature increases in downstream areas. Zhang et al.[(2)] investigated the relationship between heat wave in 2007 and upstream urbanization over the Baltimore-Washington corridor in the US using a numerical model. They found that the UHI effects over Baltimore would be 1.25 °C weaker, or reduced by 25%, without the upstream urbanization. Kang et al.[(3)] investigated the Shanghai megacity in China and concluded that the UHI leads to temperature rise in the downstream area. Masumoto et al.[(4)] examined the temperature distribution in Osaka city using observational data and concluded that strong westerly to south-westerly winds (sea breezes in the area) in the daytime transport sensible heat from the central area of the city to its eastern area. Therefore, enhancement of ventilation in Osaka city as a UHI mitigation plan may lead to an increase in temperature in the inland areas.

In this study, the influence of heat transport from the central area of Osaka city on the inland areas in mid-summer using observation data and a meteorological model was investigated. Furthermore, a sensitivity test was performed by increasing the anthropogenic heat released within Osaka city and its impact on the air temperature in the inland areas was evaluated.

2. Observational data analysis

Fig. 1 shows Osaka area, which is surrounded by mountains to the north, east, and south. The western side faces the Osaka Bay. To investigate the relationship between wind direction and high temperatures in mid-summer, we categorized the local wind system of this area into several patterns using hourly data observed at Automated Meteorological Data Acquisition Systems (AMeDAS) stations. The period investigated was July and August from 2006 to 2009. Under clear day conditions (solar radiation > 18 MJ/m^2/day and precipitation < 0.5 mm/day) two contrasting patterns were focused on: large-scale sea breeze (EW-L) days and easterly wind (EE) days. EW-L is a typical land-sea breeze circulation in this area. In this type, a small-scale sea breeze from Osaka Bay develops early in the morning and a large scale sea breeze from the Pacific Ocean overrides it in the late afternoon. The number of EW-L days was 45% of all clear

days. In the EE days, easterly winds (land breeze in this area) persist all day long in a synoptic pressure pattern. On clear days this pattern appears less frequently (7%).

Fig. 2 shows the mean diurnal temperature variations at the Osaka and Hirakata AMeDAS stations (P1 and P2, respectively; see Fig.1) for each wind pattern. P1 is located in the central area of the city. P2 is in the inland area, about 20 km to the northeast of P1; therefore, P2 is in the downstream of the sea breeze. Since the daily maximum temperature (Tmax) and the daily temperature range (Tmax–Tmin) in EW-L days are smaller than in EE days at both points, it can be inferred that the sea breezes are not necessarily associated with high inland temperatures. Fig. 3 shows the relationship between the mean wind speed in the daytime (1200–1800 LST) at P1 and the daily temperature range at P1 and P2 in EW-L days. The correlation coefficient is -0.57 and -0.38 at P1 and P2, respectively. Because the mean wind speed, which represents sea breeze strength, negatively correlates with the daytime temperature rise, it is unlikely that the heat transported from the central area causes a temperature rise in the inland areas.

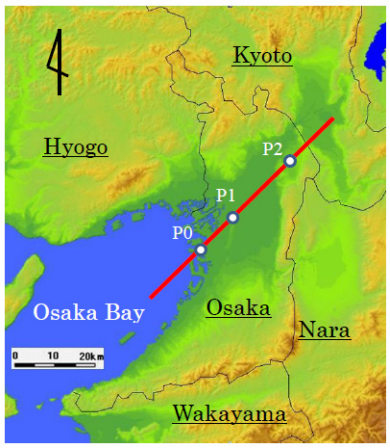

Fig. 1 Map of the study area. P1 and P2 are Osaka and Hirakata AMeDAS stations, respectively. The red line denotes the location of the vertical cross-section in Fig. 9. P0 is the point from which the distance from the coast is measured.

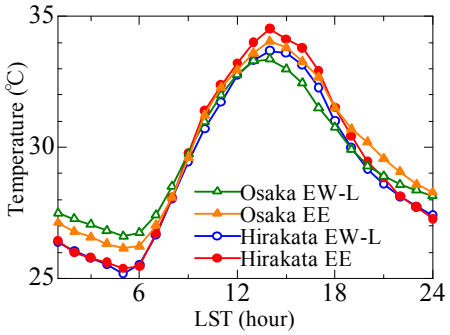

Fig. 2 Diurnal variation of mean air temperature at Osaka and Hirakata in each wind pattern in August 2006–2009.

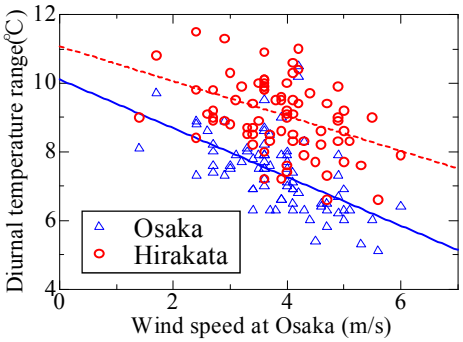

Fig. 3 Relationship between mean wind speed in the daytime (1200–1800 LST) and daily temperature range in EW-L days in August 2006–2009; solid: Osaka, dashed: Hirakata.

3. Numerical method

We used the Weather Research and Forecasting (WRF) modeling system ver.3.2.1[5] to simulate land-sea breeze circulations in the study area. The calculation parameters are shown in Table 1. Initial and boundary conditions for the meteorological variables were from the Final Operational Global Analysis database of the National Centers for Environmental Protection, with 1° resolution and 6-hour interval. Grid data of the altitude (50 m resolution) and land use (100 m resolution) were from the National Land Numerical Information database of the National and Regional Planning Bureau. A single-layer urban canopy model[6] was activated on the urban grids specified by the land use data. Fig. 4 shows the calculation domain. Two domains were set with a two-way nesting configuration. The depth of the lowest layer was about 60 m. The calculations started at 0900 LST two days before the target day. After the 39 hours spin-up, hourly data of 0100–2400 LST on Grid 2 were used for analysis.

Table 1 Calculation parameters of the numerical model.

Items	Grid1	Grid2
Grid interval (horizontal)	3.0 km	1.0 km
Number of grids (horizontal)	120×120	103×103
Number of grids (vertical)	28	
Center of grids (Lat., Lon.)	(34.672°, 135.480°)	

Each process of heat transport; i.e. advection, diffusion and radiation, was evaluated from the conservation equation of potential temperature:

$$\frac{\partial \Theta}{\partial t} = -\frac{\partial (U_j \Theta)}{\partial x_j} + \frac{\partial}{\partial x_j}\left(D_\theta \frac{\partial \Theta}{\partial x_j}\right) + \frac{\Theta}{T}\frac{1}{\rho C_p}\frac{\partial F}{\partial z}, \quad (1)$$

Total Advection Diffusion Radiation

where ρ, C_p, Θ, and T are the density, specific heat, potential temperature, and air temperature, respectively. U_j is a wind velocity component in the j direction. D_θ is the horizontal/vertical diffusion coefficient and F is the vertical radiation flux. Sensible heat flux from the ground surface was included in the diffusion term. A heating/cooling effect by condensation/evaporation of hydrometeor elements was ignored in this analysis because these processes do not contribute substantially in lower layers on a clear day.

These terms were reconstructed from the hourly outputs of the WRF model. For the reconstruction, Equation 1 was transformed into a η-coordinate system as formulated in the model, and each term was discretized according to the dynamical/physical options used in our simulation, such as an upwind scheme of 5th-/3rd-order for the horizontal/vertical advection, and the Mellor-Yamada-Nakanishi -Niino level 2.5-closure scheme for the vertical mixing. Note that instantaneous fluctuation is included in the estimated values because the evaluation is made based on the instantaneous value of hourly outputs.

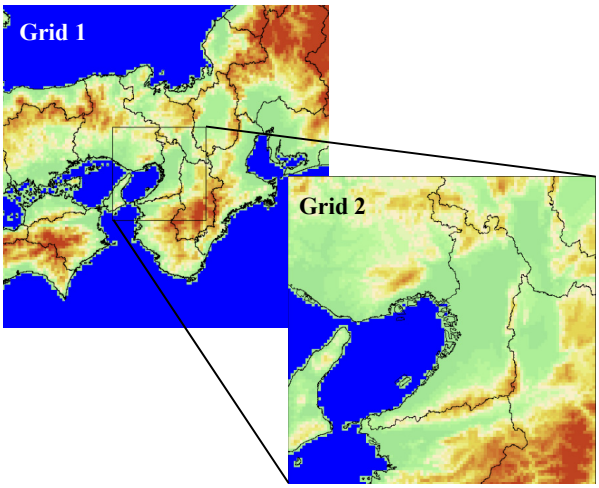

Fig. 4 Calculation domains of the numerical model.

4. Modeling results and discussion

From 2006 to 2010, several days were selected and simulated as typical days for each local circulation pattern. In the following section, the result of Aug 5, 2006 is presented as a typical EW-L condition.

4.1 Meteorological field reproduced by numerical model

The model outputs were compared with the observation data of nine AMeDAS points in Osaka prefecture. For the air temperature at 2 m, the Mean Bias Error (MBE, ≤ ±0.5 °C), Mean Absolute Error (≤ 2 °C), and Index of Agreement (IA, ≥ 0.8) are 0.32 °C, 1.10 °C and 0.96, respectively. For the wind speed at 10 m, the MBE (≤ ±0.5 m/s), Root Mean Square Error (≤ 2 m/s) and IA (≥ 0.6) are 0.51 m/s, 1.07 m/s, and 0.66, respectively. The values in the parentheses shown above are benchmarks recommended by Emery et al.[7]. The agreement is excellent because all of the benchmark indices are within the recommended values, except the MBE of wind speed, but its exceedance is very small.

Fig. 5 shows the horizontal distribution of air temperature and wind vectors at 1200 and 1800 LST. At 1200 LST, a local sea breeze arising in Osaka Bay penetrates the land. In the coastal area, the wind directions are nearly normal to the coastline. At 1800 LST, a sea breeze front can be seen deep inside the Osaka area. Since the origin of the stream is not in Osaka Bay but in the south of the analysis area (the Pacific Ocean), this stream is a large-scale sea breeze. At both times, the air temperature increases from the coast to the inland areas along the sea breeze path, i.e. air temperature is higher in the leeward side; however, it is difficult to ascertain whether this temperature gradient is caused merely by the declination of the sea breeze cooling in the inland areas or by the downstream transport of sensible heat from the central area of the city. Whether sensible heat advected by sea breezes increases air temperature in inland areas is discussed in the next section.

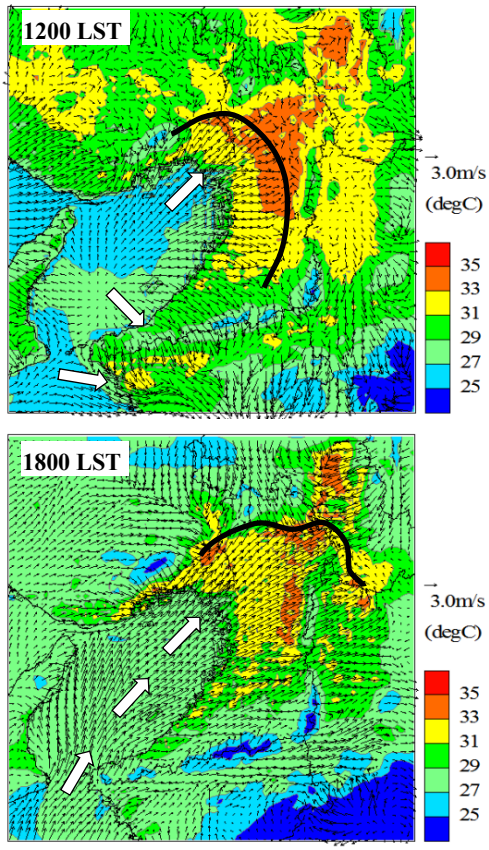

Fig. 5 Horizontal distribution of air temperature at 2 m and wind vectors at 10 m on Aug 5, 2006 (left: 1200 LST, right: 1800 LST). The thick line shows a sea breeze front and the white block arrow indicates the direction of the sea breeze.

4.2 Thermal effect of each term from the coast to inland areas

Fig. 6 shows the thermal effect of each term in the conservation equation of potential temperature in the lowest layer at 1200 and 1800 LST. The horizontal axis is distance from the coast along the red line shown in Fig. 1. As shown in Fig. 6, the diffusion term (surface heat flux) and advection term show large positive and negative values, respectively, and they almost cancel each other. At 1200 LST the change rate of potential temperature over land is determined substantially by the heating of the radiation term. The cooling effect of the advection term is more prominent at 1800 LST. The magnitude of the advection term decreases from the coast to the inland areas, but it hardly turns positive even in the inland areas; therefore, it always contributes as a cooling term and does not cause temperature rise.

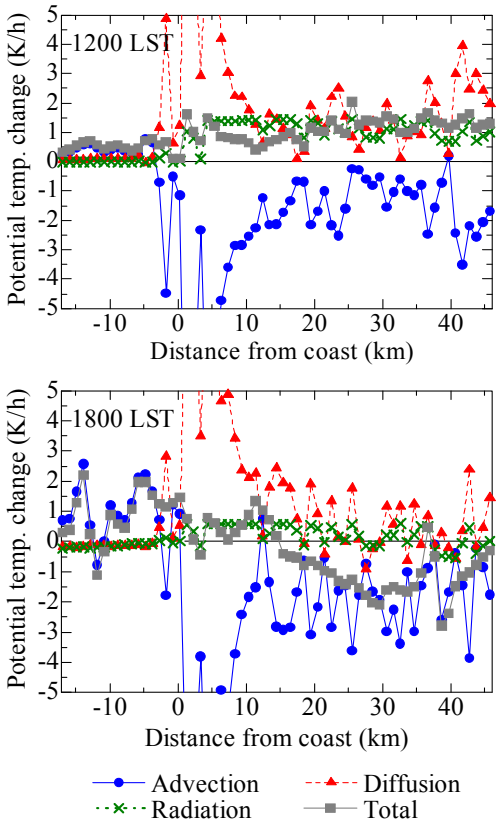

Fig. 6 Variation of each term in the conservation equation of potential temperature along the distance from the coast in the lowest layer, upper: 1200 LST, lower: 1800 LST on Aug 5, 2006.

4.3 Influence of heat transfer from the city area to the inland areas by sea breeze

To investigate how the heat generated in the central area of Osaka city affects the air temperature in the inland areas under EW-L conditions, a sensitivity analysis of hypothetical heat release was conducted. The amount of anthropogenic heat released in the entire Osaka city (see Fig.7) was increased by two times (Case 2) and three times (Case 3) that of the control case (Case 1; 90 W/m^2 at maximum).

Fig. 8 shows the difference of the daily maximum air temperature along the red line shown in Fig. 1. A large temperature difference exists only in the Osaka city area where the heat released is increased, and the maximum air temperature in the inland areas does not change much. In Fig. 8, Osaka city is 2–22 km from the coast, and a temperature rise is found within 10 km from the downwind edge of the city, but the increment is less than 0.2 °C, which corresponds to only one quarter of the value in the city area. Fig. 9 shows the distribution of the potential temperature difference (Case 2–Case1) and wind vectors of Case 1 at 1730 LST on the vertical cross section along the red line in Fig. 1. At this time, the sea breeze penetrates about 35 km from the coast, and the potential temperature difference reaches over 1000 m above the ground, which means that most of the heat released in Osaka city is diluted vertically by the passage of a sea breeze front. Additionally, the increase in the heat released in the city area causes a delay in sea breeze penetration to the downwind areas (Fig.10); therefore, it leads to a delay in temperature decrease late in the afternoon in the inland areas. Differences in the daily minimum temperature were also investigated (not shown here). Similar to the result of the daily maximum temperature, the increase in the minimum temperature was limited to the city and its vicinity.

5. Conclusion

This study confirms that sea breezes do not cause a rise in the daily maximum temperature in inland areas. Sea breeze has a cooling effect at all times. Even if anthropogenic heat released in Osaka city is greatly increased, the effect on the inland areas is very small because most of the heat is diluted vertically and the cooling effect of sea breezes is maintained. Therefore, promotion of ventilation in Osaka city to enable passage of sea breezes will not lead to temperature rise in the inland areas.

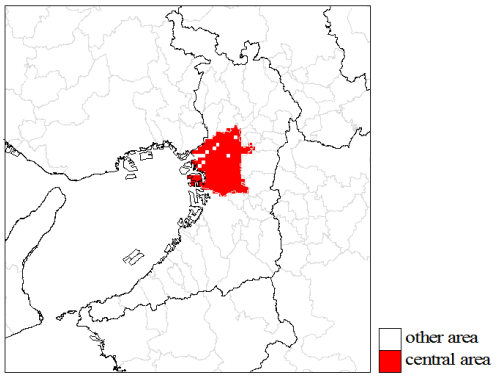

Fig. 7 Central area of Osaka city where anthropogenic heat is hypothetically increased.

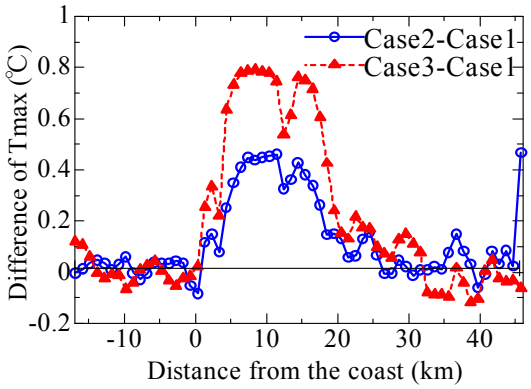

Fig. 8 Difference in the daily maximum temperature (Tmax) on Aug 5, 2006.

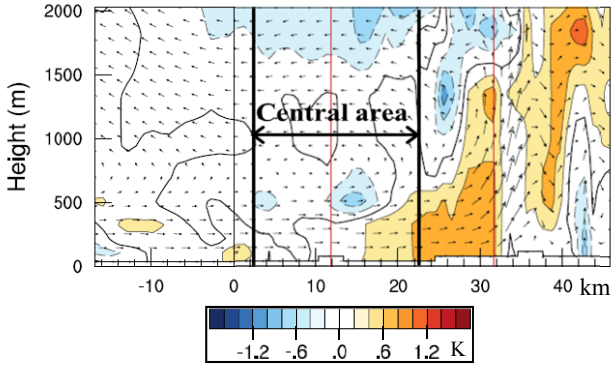

Fig. 9 Distribution of potential temperature difference (Case2–Case1) and wind vectors on a vertical cross section in Case 1 at 1730 LST on Aug 5, 2006. The cross section is along the red line shown in Fig.1.

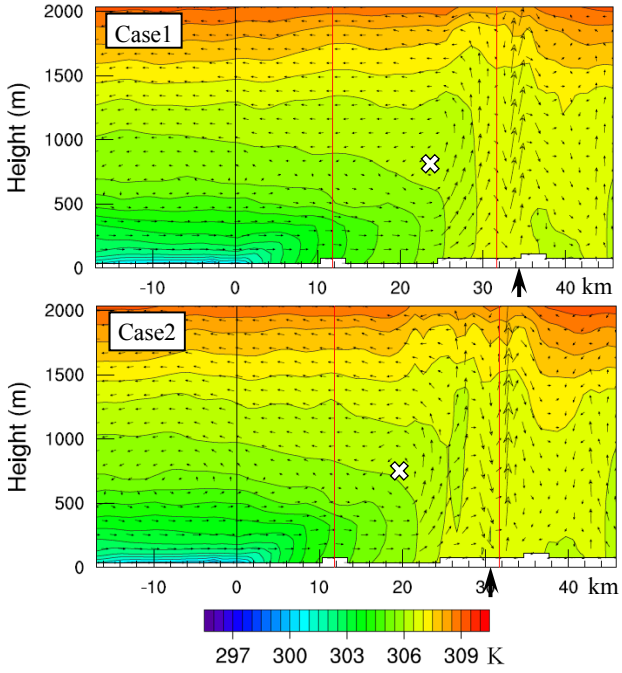

Fig. 10 Distribution of potential temperature and wind vectors on a vertical cross section at 1700 LST on Aug 5, 2006. Upper: Case1, lower: Case2. The cross section is along the red line shown in Fig.1. The white cross and a thick black arrow indicate the center of the sea breeze head and the sea breeze front near the ground surface, respectively.

References

(1) City of Osaka, *"Kaze-no-Michi" vision [Basic policy]*, available from <http://www.city.osaka. lg.jp/kankyo/page/0000123906.html> (2011), [31 March 2014].

(2) D.L. Zhang et al., *Impact of Upstream Urbanization on the Urban Heat Island Effects along the Washington–Baltimore Corridor*, J. Appl. Meteor. Climatol., **50**, 212-2019 (2011).

(3) H.-Q. Kang et al., *Impact of Megacity Shanghai on the Urban Heat-Island Effects over the Downstream City Kunshan*, Bound.-Layer Meteor. , **152**, 411-426 (2014).

(4) K. Masumoto et al., *Characteristics of Air Temperature Distribution in 2005 and Situation of Heat Island in Osaka City*, J. Heat Island Ins. Int., **1**, 30-35 (2006).

(5) W.C. Skamarock, et al., *A description of the advanced research WRF Ver.3*, NCAR Technical Note (2008).

(6) H. Kusaka: *Coupling a single-layer urban canopy model with a simple atmospheric model, Impact on urban heat island simulation for an idealized case*, J. Meteor. Soc. Japan, **82**, 1, 67-80 (2004).

(7) C. Emery et al., *Enhanced meteorological modeling and performance evaluation for two Texas ozone episodes*, Project report prepared for the TNRCC, US (2001).

(Received Dec. 12, 2014, Accepted Dec. 27, 2014)